Osteoclasts control sensory neurons axonal growth through epidermal growth factor receptor signaling

Estrela Neto[1, 2, 3], Daniela M. Sousa[1, 2], Francisco Conceição [1, 2, 4], Luís Leitão[1, 2, 4], Cecília J. Alves[1, 2], Inês S. Alencastre[1, 2], Jonathan West[5], Richard O. C. Oreffo[6] and Meriem Lamghari[1, 2, 4]*

[1]i3S - Instituto de Investigação e Inovação em Saúde, Universidade do Porto, Rua Alfredo Allen 280, 4200-135 Porto, Portugal

[2]INEB - Instituto de Engenharia Biomédica, Universidade do Porto, Rua Alfredo Allen 280, 4200-135 Porto, Portugal

[3]FMUP - Faculdade de Medicina da Universidade do Porto, Alameda Prof. Hernâni Monteiro, 4200-319 Porto, Portugal

[4]ICBAS - Instituto de Ciências Biomédicas Abel Salazar, Universidade do Porto, Rua de Jorge Viterbo Ferreira n.º 228, 4050-313 Porto, Portugal

[5]Institute for Life Sciences, University of Southampton, University of Southampton Highfield Campus, Southampton SO17 1BJ, United Kingdom

[6]Centre for Human Development, Stem Cells and Regeneration, Institute of Developmental Sciences, Tremona Rd, Southampton SO16 6YD, United Kingdom

*Correspondence:

Meriem Lamghari,

Rua Alfredo Allen 280, 4200-135 Porto, Portugal; Phone: +351 220408800; lamghari@ineb.up.pt

Abstract

Dense ectopic sprouting of nerve fibers was reported in several bone pathologies featuring high osteoclast number and/or activity. Osteoclasts play a critical role on nociceptors activation; however, their contribution to nerve fibers outgrowth is unknown. This study provides compelling evidence that osteoclastic lineage has an intrinsic capacity to promote axonal outgrowth of dorsal root ganglia (DRG), surpassing the neurotrophic potential of bone marrow stromal cells. Using microfluidic devices, we showed that osteoclast-secreted molecules induced nerve growth via local action on nerve terminals. Interestingly, the axonal outgrowth mediated by osteoclast is neurotrophin-independent but implicate epidermal growth factor receptor (EGFR)/ErbB2 signaling. Ligand search studies showed lack of EGFR agonists in osteoclast secretome, however, demonstrated an increase of endogenous EGF in DRG under osteoclast stimulation. Moreover, proteomic analysis revealed molecules able to trigger EGFR signaling to induce osteoclast-mediated axonal outgrowth, as fibronectin, low-density lipoprotein receptor-related protein 1 and periostin.

Keywords: osteoclasts; axonal growth; sensory neurons; secretome; epidermal growth factor receptor (EGFR)/ErbB2 signaling; microfluidics

Introduction

The presence of nerve fibers in the bone microenvironment has been directly implicated in bone homeostasis and bone regeneration [1–5]. Anatomical mapping of innervation during skeletal development shows co-localization of nerve fibers with a rich capillary network in areas with high osteogenic activity [6–10]. Moreover, intense sprouting of nerve fibers has been observed in injured or diseased bones [11–15]. In normal bone formation, the pattern of neuronal dynamics observed during development is typically repeated [7,16–18], highlighting the critical role of neuronal regulation. Furthermore, several denervation studies have revealed an impairment on fracture healing, emphasizing the impact of the peripheral nervous system on bone turnover [19–23].

Sensory innervation has attracted significant interest concerning bone formation. Beyond their role in bone nociception, evidence demonstrates that the lack of sensory nerves within the bone microenvironment significantly impairs bone mass accrual. Thus, sensory nerves play a key role in bone homeostasis [24,25].

Bone cells have been shown to actively respond to neural factors [26], and neural key molecules participate in bone turnover [27]. Nevertheless, it remains unclear how bone cells create or maintain a permissive environment for the presence and sprouting of nerve fibers within the skeleton microenvironment. The high neurotrophic potential of bone marrow cells is well known [28–35], although the role of osteoclasts in the modulation of nerve growth remains far from clear. Interestingly, in pathological conditions such as bone cancer where ectopic sprouting of nerve fibers in the bone marrow, mineralized bone, and periosteum occurs [11,12,14,36], osteoclasts play a major role in the activation of nociceptors. The matrix resorption in the bone compartment results in a decrease in the pH milieu as a consequence of active proton secretion into the extracellular space [37–39], stimulating the acid-sensing ions channels in nerve endings leading to pain. Notably, clinical data showed that osteoclast inhibitors significantly reduced cancer-associated bone pain [40,41].

While such studies provide support for the role of osteoclasts in the activation of nociceptors in diseased bone [42], the extent to which osteoclasts contribute to the changes in the innervation pattern in normal or diseased bone is unknown. The current study has examined the effects of the osteoclast on the growth of sensory nerve fibers. We demonstrate the paracrine effect of osteoclasts at different maturation stages on axonal outgrowth and have investigated the main signaling pathways and possible molecules involved in intercellular crosstalk.

Results

Osteoclast secretome promotes sensory neurons neurite outgrowth

Osteoclasts were differentiated from the hematopoietic lineage of bone marrow cells and the phenotype confirmed by increased expression of tartrate-resistant acid phosphatase (TRAP), cathepsin K (CTSK) and osteoclast associated immunoglobulin-like receptor (OscAR) (Figure 1A). Immunostaining revealed a large population of multinucleated osteoclasts (Figure 1B) with the low contribution of positive F4/80 macrophages present in the culture. Reactivity to TRAP also confirmed the mature osteoclast phenotype (Figure 1C).

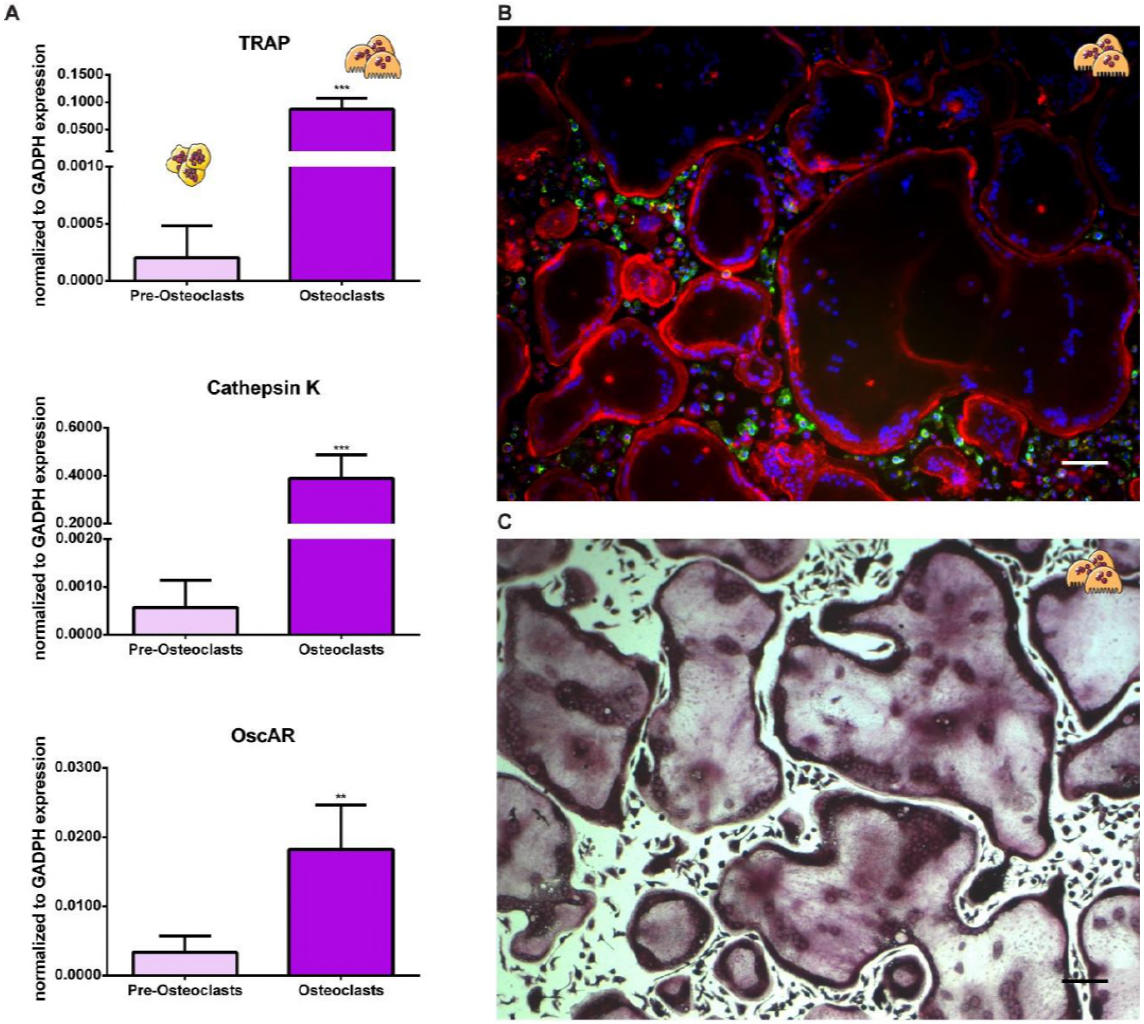

Figure 1: Characterization of osteoclasts differentiation *in vitro*. Osteoclasts were differentiated from mouse bone marrow hematopoietic lineage. **A.** Differentiation markers (tartrate-resistant acid phosphatase (TRAP), cathepsin K (CTSK) and osteoclast associated immunoglobulin-like receptor (OscAR)) were evaluated by qPCR. Data represented as mean±S.E.M. **B.** Image of multinucleated osteoclasts stained for F-actin (red), nuclei (blue) and macrophages stained with F4/80 (green). **C.** TRAP staining of mature osteoclasts differentiated *in vitro*. Scale bar 100 µm.

92 The secretome derived from osteoclast precursors (pre-OC) and mature osteoclasts (OC)
93 populations was tested on explants of embryonic dorsal root ganglia (DRG) cultures (Figure 2A).
94 Outgrowth from sensory neurons was used to assess the neurotrophic potential of differentiating
95 osteoclasts. After treatment, axonal outgrowth was calculated using a Matlab-based algorithm
96 [43]. DRG treated with osteoclastic lineage conditioned media (pre-OC and mature OC), showed
97 significantly higher axonal outgrowth when compared to the neurobasal-nerve growth factor
98 (neurobasal (+NGF)) supplemented control (Figure 2B-C). The mature osteoclast secretome
99 demonstrated an approximate 3-fold stronger influence on sensory neurons growth than the
100 secretome from bone marrow stromal cells (BMSC), previously demonstrated to have a positive
101 neurotrophic potential [33,44]. Additionally, there was a notable effect on axonal outgrowth
102 induced by the mature osteoclasts indicating an intrinsic capacity magnified with the maturation
103 stage (Figure 2B-C). Explant DRG cultures were also treated with osteoclast differentiation
104 medium (OCm) to rule out the effect of receptor activator of nuclear factor kappa-B ligand
105 (RANKL) and macrophage colony-stimulating factor (M-CSF) present in the medium known to
106 modulate axonal outgrowth [45,46]. No significant differences were observed when compared to
107 neurobasal control media (Figure 2B).

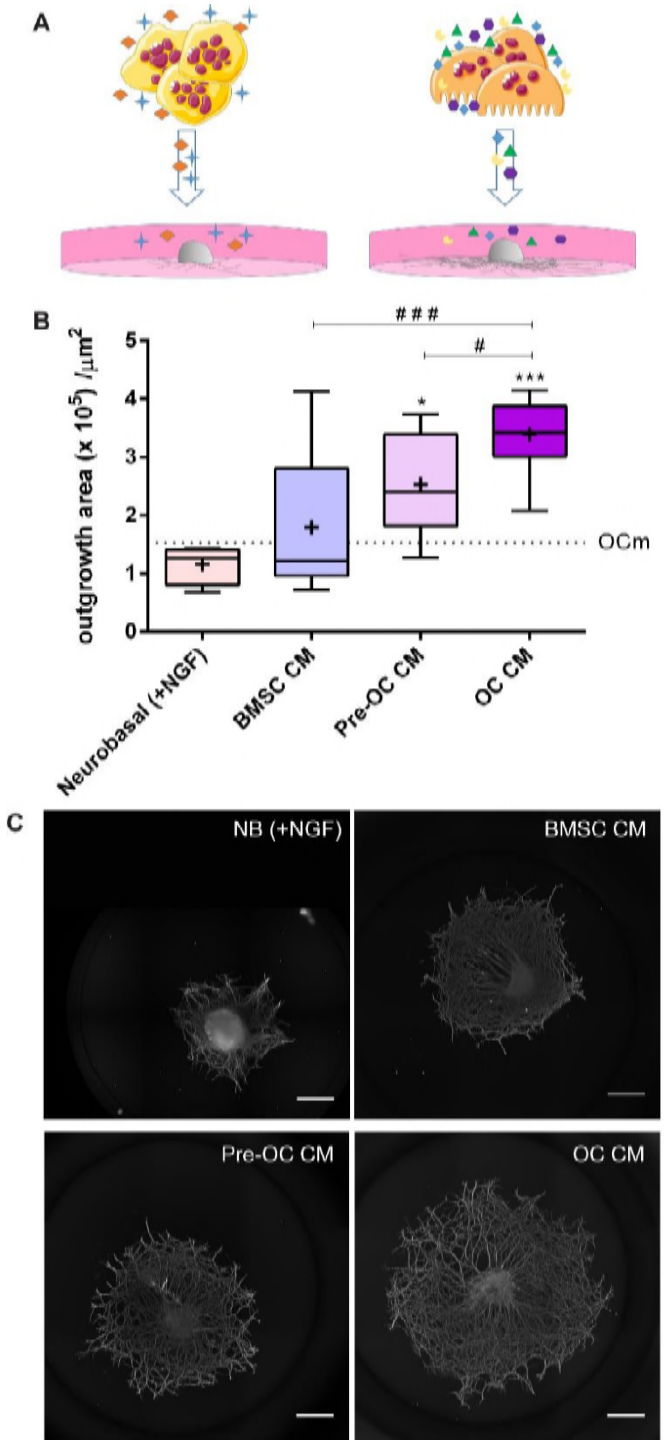

Figure 2: **Effect of osteoclasts on axonal outgrowth of sensory neurons. A.** Schematic representation of experimental setup. Pre-osteoclast conditioned media (Pre-OC CM) and mature osteoclast conditioned media (OC CM) was collected and added to embryonic DRG culture. **B.** Representative images of DRG outgrowth after treatment (stained for βIII-tubulin, scale bar 500 µm). **C.** Automatic axonal outgrowth quantification of DRG treated with Neurobasal (+nerve growth factor (NGF)), bone marrow stromal cells conditioned medium (BMSC CM), Pre-OC CM, OC CM and osteoclast medium (OCm, dashed line). Data represented as box & whiskers (line=median, +=mean). Statistical analysis was performed *vs.* controls – Neurobasal and OCm (*) and between groups (#).

In physiological conditions, the cell soma of sensory neurons is confined to the DRG and only the axonal terminals are present in the bone microenvironment. Therefore, microfluidic platforms were used to recapitulate the physical separation of soma/axonal structures with the possibility to exclusively stimulate the axonal compartment (Figure 3A). To understand the direct effect of the soluble factors released by the mature osteoclasts in the activation of receptors present in the axonal terminals, the secretome of mature osteoclasts was specifically applied to axon compartment. Neurite outgrowth was measured with AxoFluidic, an algorithm designed to quantify neurite projection within microfluidic platforms [47]. The Axofluidic calculates the exponential fit in the axonal compartment given by the spatial dependence decay function $f(x) = A\, e^{-x/\lambda}$, where χ represents the spatial variable and λ represents the scale of spatial decay (associated with the length of the neurite). The secretome of mature osteoclasts reproduced the effects observed with NGF stimulation through axonal terminals (Figure 3B-C).

These data demonstrate that local administration of osteoclast secretome on the axonal terminals of sensory neurons induced neurite outgrowth. Similar to the effect of NGF, mediated by the activation of TrkA receptors present in axonal growth cones, the effect of the osteoclast secretome could be mediated through neurotrophins present in the conditioned media and their corresponding receptors. Therefore, the neurotrophins present in the osteoclast secretome were quantified.

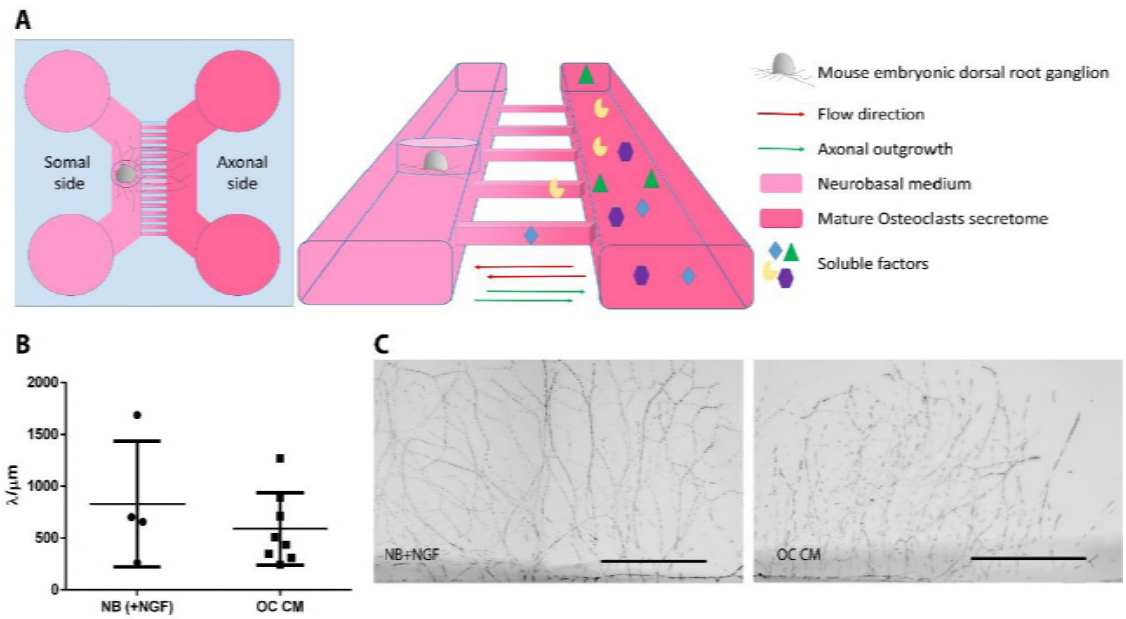

Figure 3: Axonal outgrowth in microfluidic platforms. DRG were cultured in microfluidic devices to isolate the axonal terminals from cell soma. **A.** Schematic representation of a DRG cultured on a microfluidic platform (somal side). Osteoclast secretome was specifically added to the axonal side of the chamber. **B.** Quantification of axonal projection in the axonal side using Axofluidic. λ constant, retrieved from the exponential decay function, represents the distance of the neurites projection. Data represented as scatter plot (mean±SD) **C.** Representative images of neurite

projection on axonal compartment (NB (+NGF) left and OC CM right). β III tubulin in black, scale bar = 500 µm.

Osteoclast-induced axonal outgrowth is neurotrophin-independent

Neurotrophins are classified as promoters for neuronal survival and differentiation. Four neurotrophins are known to be expressed in mammals: NGF, brain-derived neurotrophic factor (BDNF), Neurotrophin-3 (NT-3) and NT-4 [48]. Therefore, neurotrophins in the osteoclast secretome were measured to understand the contribution of these proteins in the crosstalk between osteoclasts and sensory neurons.

NGF, BDNF, NT-3 and NT-4/5 were not detected in the mature osteoclast secretome, despite our observation of higher neurite outgrowth on embryonic DRG explant cultures, while NGF and BDNF were detected in the BMSC secretome (Figure 4), as previously described in other reports [33,44]. Although previous studies by Togari *et al.* demonstrated the mRNA expression of NGF and BDNF by osteoclasts, these were not detected by ELISA or Western Blot [49].

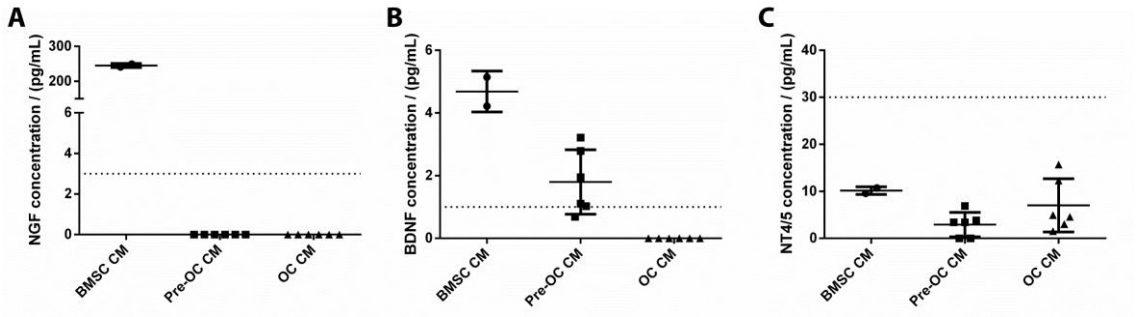

Figure 4: Analysis of neurotrophins in secretome. Quantification of NGF, BDNF, NT-3 and NT-4/5 on bone marrow stromal cells conditioned medium (BMSC CM), pre-osteoclast conditioned medium (Pre-OC) and mature osteoclast conditioned medium (OC CM). NT-3 was not detected in any condition (data not shown). The dashed line represents the limit of detection for the ELISA assay. Data represented as scatter plot (mean±SD).

In our work, we performed the screening of receptor tyrosine kinases phosphorylation, implicated in neuronal development, growth, survival and axonal regeneration [50]. Low levels of TrkA, TrkB and TrkC activation were observed further confirming the low contribution of NGF, BDNF, NT-3 and NT-4/5 neurotrophins.

Among the different phosphorylated receptors, epidermal growth factor receptor (EGFR), ErbB2, ErbB3 and platelet-derived growth factor receptor alpha (PDGFRα) displayed raised activation levels in the condition where high axonal outgrowth was observed (Figure 5A). Interestingly,

172 under osteoclast stimulation, there was an increased activation of the ErbB2 receptor in DRG
173 neurons when compared to treatment with BMSC (Figure 5B). ErbB2, an orphan receptor with no
174 characterized ligand, can be activated by spontaneous homodimer formation or by
175 heterodimerization with another ligand-bound or epidermal growth factor (EGF) family
176 transactivated receptor (Figure 5C) [51,52]. The high levels of EGFR phosphorylation indicate
177 heterodimerization of EGFR/ErbB2 leading to the pathway activation. These results are in
178 agreement with the literature where both EGFR and ErbB2 were shown to be increased in DRG
179 upon lesion, in the context of nerve repair [53]. Therefore, osteoclasts may promote axonal
180 outgrowth through EGFR family signaling, described to be involved in the neuronal repair.

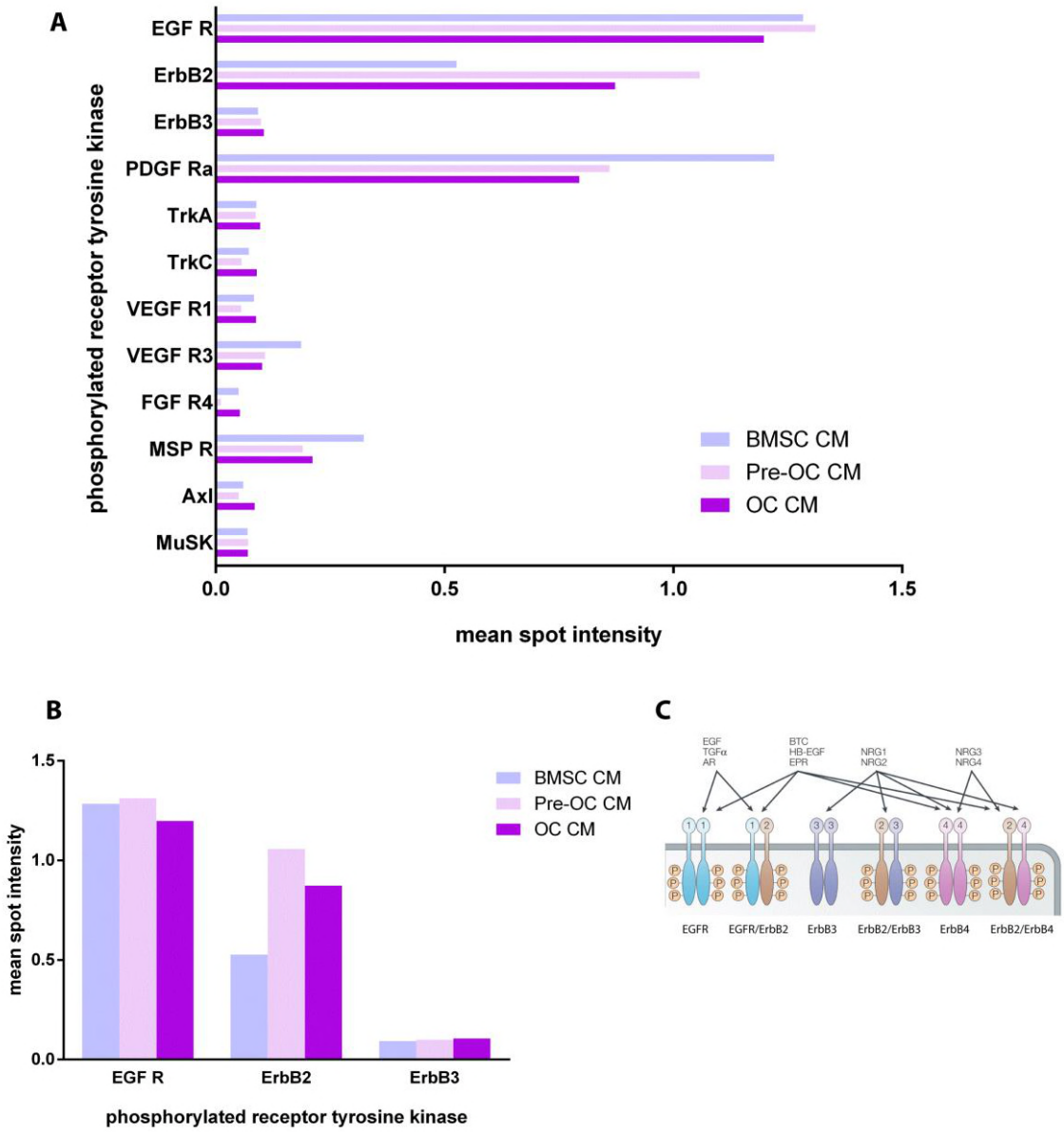

181

182 **Figure 5: Analysis of activated receptor tyrosine kinases in DRG cultures. A.** The graphic represents
183 the mean spot intensity of the most phosphorylated receptors in embryonic DRG treated with
184 different secretomes, showing the major activation of two different families: epidermal-growth

185 factor receptors (EGFR), platelet-derived growth factor (PDGF) receptor alpha. **B.** Graphic
186 highlighting the phosphorylation levels of EGFR family. **C.** Schematic representation of possible
187 EGFR family dimers formation and the correspondent ligands (adapted by permission from
188 Macmillan Publishers Ltd: Nature Reviews Cancer (61), copyright 2005).

189

190 **EGFR/ErbB2 signaling is involved in osteoclast-mediated axonal outgrowth**

191 Up to date, the effect of EGFR family activation on axonal outgrowth is not clear yet [54]. While
192 *in vivo* and *in vitro* studies showed that the inhibition of EGFR promotes axonal regeneration over
193 inhibitory environments [55–58], other studies reported that EGFR activation enhances neurite
194 outgrowth in DRG neurons [59,60].

195 To understand the contribution of EGFR and ErbB2 signaling in the osteoclast-induced axonal
196 outgrowth, two complementary approaches have been applied, one by receptor-mediated
197 inhibition using pharmacological inhibition and other by ligand searching.

198 Erlotinib is an EGFR inhibitor that reversibly binds to the intracellular tyrosine kinase domain of
199 the receptor. It is described to selectivity block the EGFR over ErbB2 but at high concentrations,
200 inhibits both receptor kinases [52,61]. Our results show that the neurotrophic effect of
201 osteoclasts was reduced in the presence of the higher tested Erlotinib concentration (100 µM)
202 (Figure 6A-B), suggesting that both EGFR/EGFR homodimers and EGFR/ErbB2 heterodimers might
203 contribute the osteoclast-mediated effect on axonal outgrowth.

204 To unravel the input of ErbB2 in osteoclast neurotrophic effect the monoclonal antibody
205 Trastuzumab® (also known as Herceptin®) was used against the extracellular domain of the
206 receptor [62]. Upon treatment with Trastuzumab®, no differences on the outgrowth area of the
207 sensory neurons were observed (Figure 6C-D), indicating that sole inhibition of ErbB2 signaling
208 fails to circumvent the osteoclast secretome stimuli. These results show that osteoclast-mediated
209 axonal outgrowth required both EGFR- and ErbB2 receptor-dependent pathways.

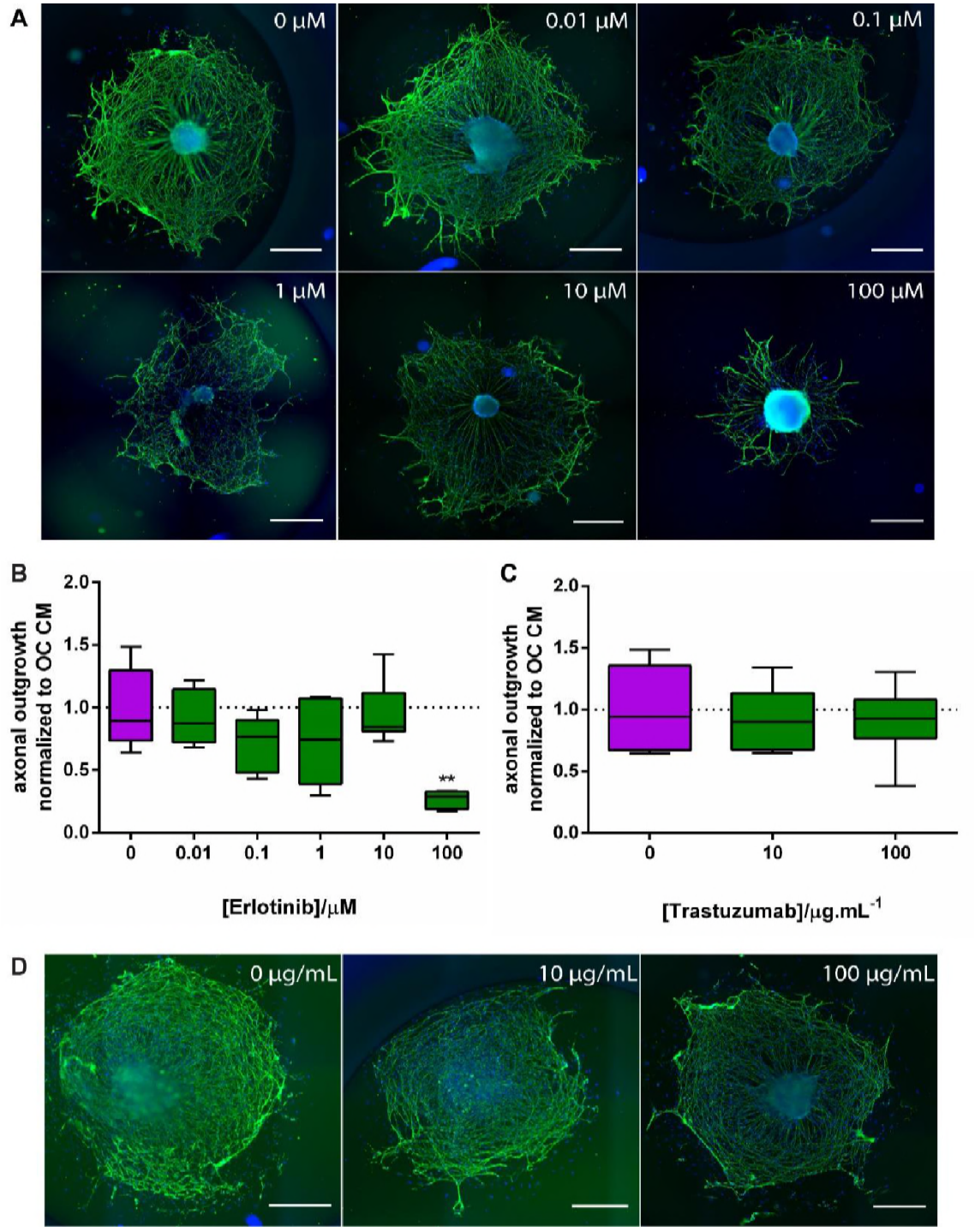

Figure 6: Pharmacological inhibition of EGFR and ErbB2. A. Representative images of DRG treated with different concentrations of Erlotinib (βIII tubulin in green and nuclei in blue, scale bar 500 µm). **B.** Quantification of axonal outgrowth of sensory neurons blocked with epidermal growth factor receptor (EGFR) inhibitor – Erlotinib. **C.** Quantification of axonal outgrowth of sensory neurons blocked with ErbB2 receptor inhibitor – Trastuzumab®. **D.** Representative images of DRG treated with different concentrations of Trastuzumab® (βIII tubulin in green and nuclei in blue, scale bar 500 µm). Data represented as box&whiskers (median).

220 Endogenous expression of EGF is triggered upon osteoclast stimulation

221 Among EGFR agonists, EGF was previously showed to mediate axonal extension in several studies
222 [59,63,64]. Thus, EGF released by osteoclasts was quantified in their secretome, and endogenous
223 EGF expression by stimulated DRG was performed by immunohistochemistry. The results showed
224 that EGF was not present in osteoclast secretome at detectable concentrations (data not shown).
225 However, immunocytochemistry analysis revealed spread localization of EGF positive staining in
226 the DRG stimulated with osteoclast conditioned medium in comparison to the control DRG
227 (neurobasal+NGF). EGF was expressed by cell soma and neurite projections of sensory neurons
228 (Figure 7B'-D', white arrows) as well as in the cells migrating from explant ganglion (Figure 7E',
229 white arrows) while the control DRG, EGF expression was confined to the core of the ganglion
230 (Figure 7A').

231 Together, these results indicate that under osteoclast stimulation, the endogenous EGF
232 expression in DRG cells can mediate the activation of the EGF signaling cascade through the
233 EGFR/EGFR and EGFR/ErbB2 dimers.

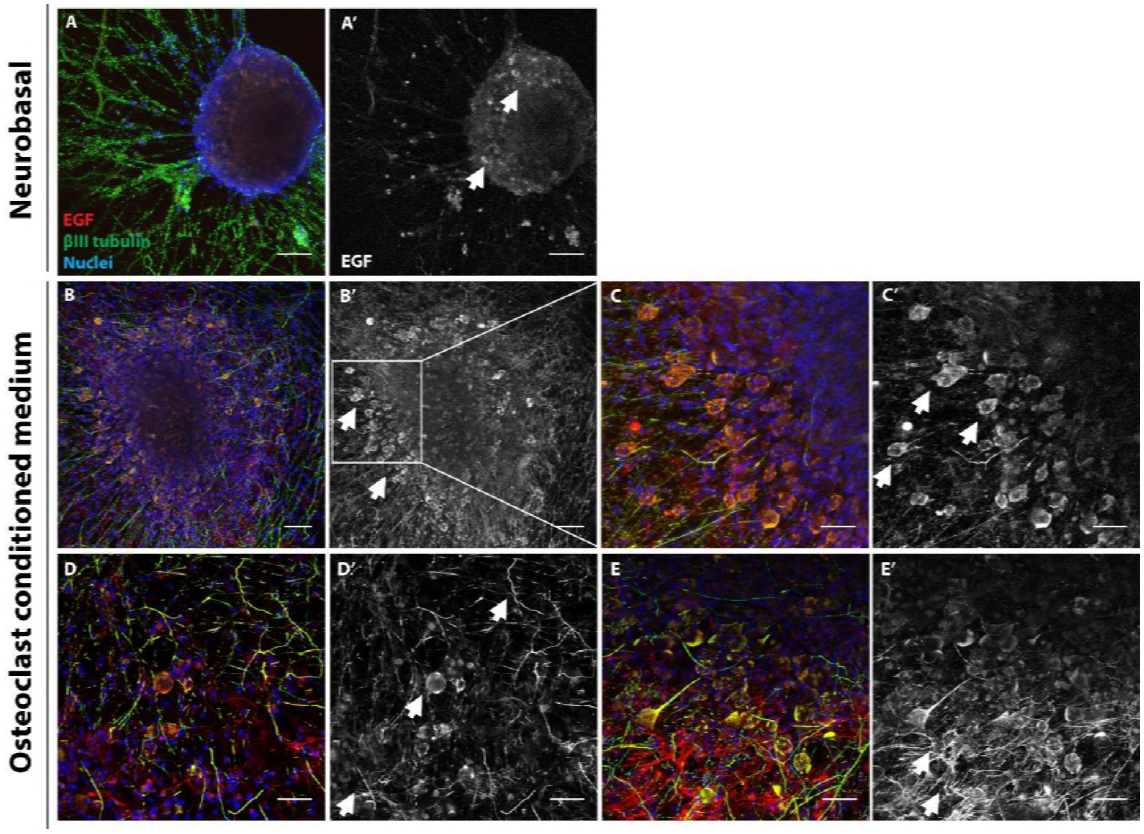

234

235 **Figure 7: Expression of epidermal growth factor (EGF) in dorsal root ganglia (DRG). A.** EGF staining
236 on DRG cultured in control conditions – neurobasal + NGF. **A'.** Isolated red channel from image A
237 showing the positive staining of EGF. **B.** EGF staining on DRG cultured with mature osteoclasts
238 conditioned medium. **C.** Zoom in from image B, showing in detail the expression of EGF in cell
239 soma of sensory neurons. **D.** Detailed image of neurites stained for EGF. **E.** Detailed image of cells

240 migrating from DRG positively stained for EGF. White arrows show positive staining (EGF in
241 red/white, βIII tubulin in green and nuclei in blue, scale bar 100 µm (A, B) and 50 µm (C-E)).

242

243 Osteoclasts soluble proteins targeting axonal outgrowth

244 To identify potential molecules mediating the osteoclast-mediated axonal outgrowth, directly or
245 indirectly, the total murine osteoclast secretome was analyzed.

246 Liquid chromatography and mass spectrometry of the osteoclast secretome identified more than
247 two hundred proteins against the *Mus musculus* database. Pro Group Algorithm software
248 calculates an unused score of 2 for a peptide with 99% identity confidence, and an unused score
249 of 1.3 for a peptide with 95% confidence level. The unused protein score, representing the sum
250 of the log confidence contributions of unique peptides used exclusively in the identification of
251 the given protein, was applied. Proteins identified with an unused score above 15 were
252 afterwards analyzed with STRING database v.10.0 and enriched for different cellular components
253 (Table S1).

254 Most of the identified proteins can be assigned to the extracellular region, mainly as components
255 of the extracellular matrix (ECM) but also from the plasma membrane. According to Gene
256 Ontology biological function terms, extracellular proteins (both ECM and secreted proteins) are
257 related to cell adhesion and five proteins appear related to nervous system development (bold
258 type in Table S1) suggesting a possible contribution of these proteins in neurite growth.

259 Among the different identified proteins, fibronectin, low-density lipoprotein receptor-related
260 protein 1 (LRP1) and periostin have been described as regulators of axon growth [65–68]. Analysis
261 of the first shell of interaction of fibronectin, LRP1 and periostin with STRING software (Figure S1)
262 identified molecular interactions with PDGF, EGFR, and TGF, which can be important for
263 osteoclasts - sensory neurons crosstalk. In fact, adhesion to fibronectin stimulates tyrosine
264 phosphorylation of the EGFR in the absence of receptor ligands [69]. Interestingly, periostin also
265 binds to the integrins αvβ3, αvβ5, and α6β4, promoting the recruitment of EGFR and the
266 activation of the Akt/PKB and FAK-mediated signaling pathways [70,71]. These results indicate
267 the presence of other molecules in the osteoclast secretome capable of activating this signaling
268 pathway.

269

270

271

272

Discussion

The present study provides compelling evidence that osteoclast lineage has a remarkable intrinsic capacity to stimulate axonal outgrowth. Furthermore, this potential is concomitant with the differentiation stage of osteoclasts and surpasses the effect of BMSC on axonal growth. Axonal terminals integrate the cues secreted by differentiating osteoclasts after local administration of osteoclast secretome using microfluidic devices. Remarkably, proteomic analysis revealed that the observed osteoclast-mediated axonal growth was not derived from the action of the classical neurotrophins such as NGF, BDNF, NT-3 and NT4/5. In addition, receptors tyrosine kinase phosphorylation analysis confirmed low levels of TrkA, TrkB and TrkC activation. Interestingly, EGFR and ErbB2 presented high levels of activation, highlighting their possible involvement in the integration of instructive cues secreted by the osteoclasts. Furthermore, inhibition of EGFR/EGFR and EGFR/ErbB2 dimers confirmed the contribution of this signaling cascade to the osteoclast-mediated axonal outgrowth. The analysis of total osteoclast secretome indicated different proteins that can be triggering the axonal outgrowth of sensory neurons, such as fibronectin, LRP1 and periostin.

Different studies point to a parallelism between osteoclast activity and sensory neurons outgrowth in physiological and pathological conditions. Several reports have described that during embryonic long bone development osteoclasts are found in the process of endochondral ossification, degrading the new formed trabecular bone, creating the bone marrow space [72]. In another hand, longitudinal studies on the innervation process showed nerves appearing in areas with high osteogenic and chondrogenic activity during the embryonic development [6,73,74]. Thus, the presence of osteoclasts in stages where innervation process occurs suggests a latent role of these cells in the innervation pattern. In bone pathologies with increased osteoclasts number: Paget's disease [75], fibrous dysplasia [76], *osteogenesis imperfecta* [77], and with increased osteoclast activity: osteoporosis and metastatic bone disease, are frequently associated with activation of sensory nerves [78–80]. Although the pattern of innervation in these pathological conditions has been only described in metastatic bone disease, where an exuberant sprouting of sensory nerve fibers has been reported, several studies indicate osteoclasts play a fundamental role in bone pain [38,42,79,81]. Our finding that osteoclasts hold notable effect on axonal outgrowth strength the reported parallelism between osteoclast lineage and the bone innervation process and support the possibility that osteoclasts might contribute actively to the dynamics of bone innervation pattern in physiological or pathological conditions.

305 Immunohistological studies described osteoclasts in close contact with nerve fibers within bone
306 microenvironment though typical synapses were not detected in the nerve endings [9,82,83]. Yet,
307 osteoclasts are described to activate nociceptors in nerve endings through acid-sensitive
308 nociceptors that innervate the marrow, mineralized bone, and periosteum [14,38]. These
309 channels are sensitized and excited by a decrease in pH, which is generated by osteoclasts activity
310 [81,84]. Using compartmentalized microfluidic devices resembling the compartmentalized bone
311 microenvironment, where only the nerve terminals are present, we show that the osteoclast-
312 mediated axonal growth was achieved by the ability of neurite terminals to integrate, through
313 receptors, the cues secreted by differentiating osteoclasts. The most probable candidate would
314 be TrkA receptors, well known to be activated, in permissive axonal growth and regeneration
315 [48,85]. Surprisingly, tyrosine kinase receptors phosphorylation analysis performed on DRG under
316 osteoclast secretome stimulation showed that neurotrophins receptor family (TrkA/ TrkB/ TrkC)
317 were not activated. These data corroborate with the lack of their universal ligands (NGF, BDNF,
318 NT-3 or NT4/5) in osteoclast secretome demonstrated by ELISA and further confirmed by mass
319 spectrometry.

320 In the bone microenvironment, BMSC and cells of the hematopoietic lineage have been described
321 to enhance axonal outgrowth through different signaling pathways. It is known that BMSC
322 stimulate the neuron survival and neurite outgrowth of spinal or DRG neurons [34,44,86–92], and
323 were reported to produce NGF, BDNF, basic fibroblast growth factor (bFGF), glial cell line-derived
324 neurotrophic factor (GDNF), vascular endothelial growth factor (VEGF) and ciliary neurotrophic
325 factor (CNTF) to stimulate neurite outgrowth *in vitro* [33,44,86]. The macrophages, which share
326 common progenitors with osteoclasts, were shown to play a supportive role in axonal
327 regeneration and outgrowth [93,94]. M1 and M2 macrophages have divergent secretory
328 repertoires and induce different responses on axonal behavior, being the M2 macrophages
329 predominantly neuroprotective and promoters of axon growth [95,96]. The macrophages were
330 shown to enhance neurite extension through the action of granulocyte-colony stimulating factor
331 [97] or by activating calcium/calmodulin kinase-dependent pathways [98]. Herein we show that
332 the osteoclasts operate via different secreted factors and target different signaling, mainly EGFR
333 family, to promote axonal outgrowth.

334 EGFR activation is involved in neuron differentiation and survival and has been implicated in
335 responses to neuronal damage [53,59,60,99]. Nevertheless, there is an extensive discussion in
336 the literature about the direct involvement of EGFR activation/inhibition on axonal regeneration
337 [54,57,100,101]. EGFR phosphorylation has been implicated in signaling inhibition of axonal
338 growth in central nervous system [54,55,57]. Koprivica *et al.* showed that EGFR inhibitors

339 effectively promoted neurite outgrowth from cultured DRG [55]. Nevertheless, others reported
340 that EGFR knockdown did not induce neurite outgrowth of retinal ganglion cells and inhibitors of
341 EGFR showed to enhance neurite outgrowth in the absence of the receptor [54]. We and others
342 previously demonstrated an increased expression of EGFR family in DRG after lesion [53,99,102].
343 To understand the contribution of EGFR and ErbB2 signaling in the osteoclast-induced axonal
344 outgrowth, two complementary approaches were applied, one by receptor-mediated inhibition
345 using pharmacological inhibition and other by ligand searching. Our data indicate that the EGFR
346 signaling has a role in axonal outgrowth promoted by osteoclast secretome. Upon EGFR inhibition
347 with Erlotinib, described to inhibit both EGFR and ErbB2 receptor kinases at high concentrations
348 [52], we observed a significant reduction in the axonal outgrowth area. These findings are
349 consistent with prior observations that the phosphorylation of EGFR was showed to enhance
350 neurite outgrowth [59,60,63,103–105]. The EGFR-mediated axonal outgrowth, in the absence of
351 EGFR ligands from the osteoclast secretome, leads us to hypothesize that endogenous expression
352 of EGF, by the neurons and glial cells from DRG explant cultures, could occur. In fact, we showed
353 that EGF was endogenously expressed by DRG cells in culture upon exposure to osteoclast
354 secretome and, therefore, having an autocrine/paracrine effect on the activation of EGFR
355 signaling pathway. It remains to be deciphered which molecules present in the osteoclast
356 secretome can directly influence either the endogenous expression of EGF and the activation of
357 EGFR family.

358 Notably, from the total secretome analysis, other proteins described to promote axonal
359 outgrowth and activate EGFR signaling pathway were identified such as fibronectin, LRP1 and
360 periostin. Adhesion to fibronectin stimulates tyrosine phosphorylation of the EGFR in the absence
361 of receptor ligands [69]. Periostin, also detected in the osteoclast secretome, was shown to
362 promote neurite outgrowth in cerebellar granule neuron and DRG neurons [67,68] and to recruit
363 the EGFR, supporting its possible role on EGFR modulation [70]. LRP1 was hypothesized to
364 promote axonal sprouting and regeneration in the adult central nervous system by activation of
365 canonical signaling pathways associated with neurotrophin receptors [66]. These molecules
366 present in the osteoclast secretome can directly influence the activation of EGFR signaling
367 cascade. Moreover, others can act directly on neurons or glial cells to induce the endogenous
368 expression of EGF. Some authors claimed that the effect of EGF on axonal outgrowth might be an
369 off-target effect. EGF can act on glial cells to increase the expression of neurotrophins and,
370 consequently, intensify the axonal outgrowth [100,106]. In line with these observations, the glial
371 cells at the explant culture can be producing neurotrophins upon osteoclast secretome

372 stimulation to improve the neurite outgrowth. Nevertheless, the TrkA, TrkB and TrkC receptors
373 did not show high phosphorylation levels.

374 In conclusion, our data provide robust evidence of the neurotrophic potential of the osteoclastic
375 lineage on axonal outgrowth, delivering new insights into the crosstalk between osteoclasts and
376 sensory neurons. Clearly, besides the activation of nociceptors through microenvironment
377 acidification, osteoclasts and their secreted molecules can be implicated in cancer-associated
378 bone pain possibly through the control of nerve sprouting and consequently remodeling of the
379 pathological innervation pattern. This is a subject that deserves further investigation to i)
380 control/reduce the formation of neuroma-like structures and ii) specify new candidates as
381 potential targets for bone pain therapies.

382

383 Materials and methods

384 All animal procedures were approved by the IBMC/INEB ethics committee and by the Portuguese
385 Agency for Animal Welfare (*Direção-Geral de Alimentação e Veterinária*) in accordance with the
386 EU Directive (2010/63/EU) and Portuguese law (DL 113/2013). Mice were housed at 22 °C with a
387 12 h light/dark cycle with *ad libitum* access to water and food. Adult C57Bl/6 male mice (6-8
388 weeks-old) were sacrificed in a carbon dioxide chamber to obtain bone marrow cells, while
389 pregnant females were sacrificed by cervical dislocation.

390

391 Cell culture

392 Bone marrow cells cultures

393 Bone marrow cells were isolated from tibiae and femur by flushing the bone marrow with α-MEM
394 (Gibco, Thermo Fisher Scientific, Waltham, MA, USA) containing 10% (v/v) heat inactivated (30
395 min at 56 °C) foetal bovine serum (FBS, Gibco, Thermo Fisher Scientific) and 1% (v/v)
396 penicillin/streptomycin (P/S, Gibco, Thermo Fisher Scientific). Non-adherent cells were removed
397 after 3 days and fresh medium was added. After three days the conditioned medium was
398 collected, centrifuged at 140 g, 4 °C, 5 min and stored at -80 °C. The conditioned medium was
399 divided into small aliquots (500 µL - 1 mL) before freezing to avoid repeated freeze/thaw cycles.

400

401

402 Osteoclast cultures

403 Bone marrow cells were isolated from tibiae and femur by flushing the bone marrow with α-MEM
404 containing 10% (v/v) FBS and 1% (v/v) P/S. To generate primary osteoclast precursors, the bone
405 marrow mononuclear cell suspension was treated with red blood cells lysis buffer (ACK lysing
406 buffer, #A1049201, Gibco, Thermo Fisher Scientific) for 1 min at room temperature (RT) and, after
407 centrifugation, cells were plated in 10-cm-diameter Petri dishes with 10 ng/mL macrophage
408 colony-stimulating factor (M-CSF, PeproTech, London, UK) for 24 h. Afterwards the M-CSF
409 concentration was increased to 30 ng/mL for an additional three days (pre-osteoclasts).
410 Conditioned medium from osteoclasts precursors was collected, centrifuged at 140 g, 4 °C, 5 min
411 and stored at -80 °C. Adherent cells were then detached with a cell scrapper and seeded at a
412 density of 5 x 10^4 cells/cm^2 in the presence of 30 ng/mL M-CSF and 100 ng/mL receptor activator
413 of nuclear factor kappa-B ligand (RANKL, PeproTech) [107,108]. Cells were maintained at 37 °C in
414 a humidified atmosphere of 5% CO_2 for 3-4 days and then osteoclast conditioned medium was
415 collected and stored at -80 °C.

416 Evaluation of osteoclast differentiation

417 Evaluation of osteoclast differentiation was performed by qRT-PCR analysis. RNA was isolated and
418 purified as previously described in [102] and the mRNA expression of differentiation markers
419 (tartrate-resistant acid phosphatase (TRAP, Fw: CGACCATTGTTAGCCACATACG; Rv:
420 TCGTCCTGAAGATACTGCAGGTT, Invitrogen, Carlsbad, CA, USA), cathepsin K (CTSK, Fw:
421 ATATGTGGGCCAGGATGAAAGTT; Rv: TCGTTCCCCACAGGAATCTCT, Invitrogen), osteoclast
422 associated immunoglobulin-like receptor (OscAR, Fw: TGGCGGTTTGCACTCTTCA; Rv:
423 GATCCGTTACCAGCAGTTCCAGA, Invitrogen) and glyceraldehyde 3-phosphate dehydrogenase
424 (GAPDH, Fw: GCCTTCCGTGTTCCTACC; Rv: AGAGTGGGAGTTGCTGTTG, Invitrogen) was
425 performed.

426 Immunocytochemistry was performed to assess the morphology of the differentiated osteoclasts
427 and the possible presence of macrophages in culture. Briefly, cells were fixed with 4%
428 paraformaldehyde (PFA, Merck Millipore, Kenilworth, NJ, USA) in phosphate-buffered saline (PBS)
429 during 10 min followed by permeabilization with 0.25% (v/v) Triton X-100 (Sigma-Aldrich, St.
430 Louis, MO, USA) in PBS and incubated, for 30 min at RT, with blocking solution composed of 1%
431 (w/v) Bovine Serum Albumin (BSA, Sigma-Aldrich) in PBS for 30 min at RT to block antibody
432 unspecific binding. The cells were incubated with macrophages specific marker – anti-F4/80 (#14-
433 4801-85, eBioscience, Thermo Fisher Scientific), 1:250 in blocking solution overnight at 4 °C.
434 Afterwards cells were washed with PBS and incubated with Alexafluor 488-Phalloidin (Life

435 Technologies, Thermo Fisher Scientific) 1:100 in PBS for 30 minutes at RT in the dark. At the end
436 of the incubation time, the cells were washed with PBS and mounted using Vectashield with DAPI
437 (Vector Labs, Burlingame, California, USA). Images were captured using the Inverted Fluorescence
438 Microscope (Zeiss AxioVert, Carl Zeiss, Oberkochen, Germany), equipped with AxioVision SE64
439 Rel. 4.8 software. TRAP staining was also performed using an Acid phosphatase, Leukocyte (TRAP)
440 kit (Sigma-Aldrich) according to manufacturer's instructions. Images were acquired using a
441 stereomicroscope (SZX10, Olympus, Shinjuku, Tokyo, Japan) coupled to a digital camera (DP21,
442 Olympus).

443

444 Dorsal root ganglia (DRG) culture

445 Embryonic DRG were obtained from 16 to 18 days-old (E16-18) murine embryos. Pregnant female
446 mice were exposed to isoflurane by inhalation. The embryos were harvested and maintained on
447 ice-cold Hank's balanced salt solution (HBSS, Invitrogen). Embryonic ganglia were accessed
448 through the dorsal side of the embryo after spinal cord removal. The meninges were cleaned
449 from the isolated DRG and the roots were cut. The ganglia were kept in cold HBSS until seeding.
450 DRG were isolated under the stereoscopic magnifier and seeded into the lower wells of a 15-well
451 µ-Slide Angiogenesis plate (#81506, Ibidi, Martinsried, Germany). Fibrin hydrogels were formed
452 in the plates by applying equal volumes of a solution of plasminogen-free fibrinogen, pooled from
453 human plasma, and a thrombin solution containing $CaCl_2$ and aprotinin (final concentration of
454 fibrin components: 6 mg/mL fibrinogen (Sigma-Aldrich); 2 NIH U/mL thrombin from human
455 plasma (Sigma-Aldrich); 2.5 mM $CaCl_2$ (Sigma-Aldrich); 10 µg/mL aprotinin (Sigma-Aldrich)).
456 Before being used in the preparation of fibrin gels, fibrinogen was dissolved in ultrapure water,
457 dialyzed against tris-buffered saline (TBS, pH 7.4), sterile-filtered and diluted to 12 mg/mL with
458 sterile TBS. The fibrin gel was allowed to polymerize for 30 min at 37 °C in a 5% CO_2 humidified
459 incubator, before the addition of culture media. DRG were cultured with neurobasal medium
460 supplemented with 2% v/v B-27 Serum-Free Supplement® (B-27, Invitrogen), 60 µM 5-fluoro-2'-
461 deoxyuridine (FDU, Sigma-Aldrich), 25 mM glucose (Sigma-Aldrich), 1 mM pyruvate (Sigma-
462 Aldrich), 50 ng/mL 7S Nerve Growth Factor (NGF, Calbiochem, Merck Millipore), 2 mM glutamine
463 (BioWittacker, Lonza, Basel, Switzerland) and 1% penicillin/streptomycin (P/S). Embryonic DRG
464 explant cultures were left undisturbed for 24 h. Afterwards, neurobasal media was replaced by
465 the conditioned media collected from BMSC and osteoclast cultures at different stages of
466 differentiation for additional three days. Controls with neurobasal supplemented with NGF and
467 α-MEM supplemented with M-CSF and RANKL (no contact with cells) were performed.

468 Osteoclast conditioned medium was also tested on axonal terminals of embryonic DRG cultured
469 using microfluidic devices. Briefly, microfluidic devices acquired from Merck Millipore were
470 modified and assembled as described in [47], to allow the alignment of the ganglia with the
471 microgrooves. Upon DRG plating, the somal side of the microfluidic chamber containing the DRG,
472 was cultured with neurobasal medium supplemented with NGF whereas the axonal compartment
473 was treated with mature osteoclast conditioned medium. Fluidic isolation was achieved by
474 maintaining the volume difference between the two compartments during 48 h, after which
475 axonal outgrowth was quantified.

476

477 Quantification of axonal growth

478 Axonal outgrowth was quantified after 72 h of treatment with conditioned medium and controls.
479 The embryonic DRG samples were fixed with 2% PFA in PBS during 10 min followed by 10 min at
480 37 °C with 4% of PFA in PBS with 4% sucrose. Ganglia were permeabilized with 0.25% (v/v) Triton
481 X-100 in PBS and incubated, for 30 min at RT, with blocking solution composed of 5% v/v normal
482 goat serum (Invitrogen) and 5% v/v FBS in PBS. DRG cultures were incubated with an antibody
483 directed against the neuronal specific marker βIII tubulin (Promega, Madison, WI, United States)
484 diluted 1:2000 in blocking solution, overnight at 4 °C. Afterwards, cells were washed and
485 incubated 1 h at RT with secondary antibody (Alexafluor 488/568, Invitrogen). Images were
486 captured either with a confocal laser scanning microscope (CLSM) Leica SP2 AOBS SE equipped
487 with LCS 2.61 software (Leica Microsystems, Wetzlar, Germany) at the i3S Advanced Light
488 Microscopy Unit or with an IN Cell Analyzer 2000 equipped with IN Cell Investigator software (GE
489 Healthcare, Little Chalfont, UK) at the i3S BioSciences Screening Unit. Radial outgrowth, defined
490 as the area between the ganglion edge and the outgrowth front, was determined. The outgrowth
491 area was computed according to Bessa *et al.* [43]. To quantify the axonal outgrowth in the
492 microfluidic platforms, neurite outgrowth was measured with AxoFluidic, an algorithm designed
493 to quantify neurite projection within these platforms [47].

494

495 Quantification of neurotrophins in secretome by enzyme-linked immunosorbent assay (ELISA)

496 Conditioned media from osteoclasts and BMSC were concentrated 10 times by centrifugation at
497 4000 g for 45 min, using 3 kDa MW cut-off filter units (Merck Millipore). In order to detect and
498 quantify the amount of NGF, brain-derived neurotrophic factor (BDNF), neurotrophin-3 (NT-3)

499 and NT4/5 in the conditioned medium, a multi-neurotrophin rapid screening ELISA kit (#BEK-
500 2231, Tebu-bio, France) was used according to the manufacturers' protocol.

501

502 Analysis of activation of Phospho-Receptor Tyrosine Kinase (RTK)

503 A proteome profiler mouse phospho-RTK array kit (#ARY014, R&D system, Minneapolis, MN, USA)
504 was used to quantify the phosphorylation level of 39 tyrosine kinase receptors, according to the
505 manufacturer's instructions. Protein lysate of DRG treated with conditioned medium was
506 analyzed. Each array membrane was exposed to X-ray film using a chemiluminescence detection
507 system (Amersham, GE Healthcare). The film was scanned using Molecular Imager GS800
508 calibrated densitometer (Bio-Rad, Hercules, CA, USA) and pixel density was quantified using
509 Quantity One 1-D Analysis Software, v 4.6 (Bio-Rad).

510

511 Pharmacological inhibition of epidermal growth factor receptor (EGFR) and ErbB2

512 Embryonic DRG were cultured in 15-well slides as previously described. Erlotinib, an EGFR
513 inhibitor, was added to the conditioned medium at 10 nM, 100 nM, 1 µM, 10 µM and 100 µM
514 and tested on DRG cultures during 72 h. Trastuzumab (Herceptin®), a monoclonal antibody
515 against the ErbB2 receptor, was kindly donated by the Instituto Português de Oncologia do Porto
516 (IPO, Porto, Portugal). Trastuzumab was tested in DRG cultures at a concentration of 10 µg/mL in
517 conditioned medium. Afterwards, axonal outgrowth was measured as previously described.

518

519 Immunostaining of EGF in explant DRG upon osteoclast secretome treatment

520 DRG exposed to osteoclast secretome were stained for EGF expression. Explant cultures were
521 fixed and permeabilized as above-mentioned. DRG were incubated with EGF primary antibody
522 (#06-102, Merck Millipore) diluted 1:400 and βIII tubulin diluted 1:2000 in blocking solution,
523 overnight at 4 °C. Afterwards, cells were washed and incubated 1 h at RT with secondary antibody
524 (Alexafluor 568/488, Invitrogen). Images were captured with a CLSM Leica SP5 AOBS SE equipped
525 with LCS 2.61 software.

526

527

528 Analysis of total secretome of mature osteoclast by information dependent acquisition (IDA) / liquid
529 chromatography – mass spectrometry (LC-MS)

530 To reduce the amount of abundant proteins (such as albumin from bovine serum) and increase
531 the signal from low abundance proteins (such as cytokines and growth factors), ProteoMiner kit
532 (BioRad) was used. Conditioned media collected from mature osteoclasts cultures, was
533 concentrated 10 times by centrifugation at 4000 g for 15 min, using 30 kDa MW cut-off filter units
534 (Merck Millipore). Protein was quantified and then digested with trypsin. After reduction (DTT,
535 10 mM, 40 min, 56 °C) and alkylation (IAA, 20 mM, 30 min in the dark, RT, 18–20 °C), overnight
536 digestion with trypsin (trypsin:sample = 1:50) was performed followed by a second in-solution
537 trypsin digestion (3 h) in 80% (v/v) acetonitrile (trypsin:sample = 1:100).

538 Protein samples were analyzed by Nano LC–MS using Triple TOF 6600 (ABSciex, Framingham, MA,
539 USA). External calibration was undertaken using a beta-galactosidase digest (ABSciex). The mass
540 spectrometer was set for IDA scanning full spectra (400–2000 m/z) for 250 ms. The top 40 ions
541 were selected for subsequent MS/MS scans (150–1800 m/z for 50 ms each) using a total cycle
542 time of 2.3 s. The selection criteria for parent ions included a charge state between +2 and +5,
543 and counts above a minimum threshold of 125 counts per second. Ions were excluded from
544 further MS/MS analysis for 12 s. Fragmentation was performed using rolling collision energy with
545 an energy spread of 5. Data were acquired with the Analyst software TF 1.7 (ABSciex,
546 Framingham, MA, USA). Proteins were identified from the raw MS and MS/MS data using Protein
547 Pilot Software v. 5.0 (ABSciex). A search was performed against the SwissProt protein database
548 with taxonomic restriction to *Mus musculus* (release 2017_03). Protein identification was
549 considered with an unused score greater than 1.3 (95% confidence). An independent false
550 discovery rate (FDR) analysis using the target-decoy approach provided with the Protein Pilot™
551 software was used to assess the quality of the identifications.

552 LC-Triple TOF MS protein identification was performed at UniMS – Mass Spectrometry Unit,
553 iBET/ITQB-UNL, Oeiras, Portugal.

554

555 Statistical analysis

556 All experiments were run in triplicate and repeated at least three times. Data analysis was
557 performed using the Mann-Whitney U test in GraphPad Prism 6.00 for Windows (GraphPad
558 Software, San Diego CA, USA). Differences between groups were considered statistically
559 significant when *$p<0.05$, **$p<0.01$, ***$p<0.001$.

Acknowledgments

The authors would like to acknowledge Maria José Oliveira and José Carlos Machado groups from i3S for the EGF antibody and Erlotinib, respectively.

This article is a result of the project NORTE-01-0145-FEDER-000012, supported by Norte Portugal Regional Operational Programme (NORTE 2020), under the PORTUGAL 2020 Partnership Agreement, through the European Regional Development Fund (ERDF). This work was also financed by Fundo Europeu de Desenvolvimento Regional (FEDER) funds through the COMPETE 2020 - Operational Programme for Competitiveness and Internationalisation (POCI), Portugal 2020, and by Portuguese funds through Fundação para a Ciência e a Tecnologia (FCT) / Ministério da Ciência, Tecnologia e Inovação in the framework of the project "Institute for Research and Innovation in Health Sciences" (POCI-01-0145-FEDER-007274) and in the framework of the financed project PTDC/BIMMED/4041/2014. EN, FC and LL are recipients of Ph.D. fellowships (SFRH/BD/81152/2011, SFRH/BD/128771/2017 and SFRH/BD/109686/2015, respectively). ISA and DMS are recipients of Post-Doc fellowships (SFRH/BPD/75285/2010 and SFRH/BPD/115341/2016, respectively).

LC-Triple TOF MS protein identification was performed at UniMS – Mass Spectrometry Unit, iBET/ITQB-UNL, Oeiras, Portugal.

The authors declare no competing interests.

Author contributions

Conceptualization, E.N. and M.L.; Methodology, E.N., D.M.S and F.C.; Investigation, E.N., D.M.S, F.C. and L.L.; Writing – Original Draft, E.N. and M.L.; Writing – Review & Editing, all authors; Funding Acquisition, M.L.; Supervision, R.O.C.O., J.W. and M.L.

References

1. Chenu C (2004) Role of innervation in the control of bone remodeling. *J Musculoskelet Neuronal Interact* **4**: 132–134.

2. Chenu C, Marenzana M (2005) Sympathetic nervous system and bone remodeling. *Jt Bone Spine* **72**: 481–483.

3. Patel MS, Elefteriou F (2007) The new field of neuroskeletal biology. *Calcif Tissue Int* **80**:

590 337–347.

591 4. Elefteriou F, Campbell P, Ma Y (2014) Control of bone remodeling by the peripheral
592 sympathetic nervous system. *Calcif Tissue Int* **94**: 140–151.

593 5. Elefteriou F (2008) Regulation of bone remodeling by the central and peripheral nervous
594 system. *Arch Biochem Biophys* **473**: 231–236.

595 6. Sisask G, Silfverswärd C-J, Bjurholm A, Nilsson O (2013) Ontogeny of sensory and
596 autonomic nerves in the developing mouse skeleton. *Auton Neurosci* **177**: 237–243.

597 7. Hukkanen M, Konttinen YT, Santavirta S, Paavolainen P, Gu X-H, Terenghi G, Polak JM
598 (1993) Rapid proliferation of calcitonin gene-related peptide-immunoreactive nerves
599 during healing of rat tibial fracture suggests neural involvement in bone growth and
600 remodelling. *Neuroscience* **54**: 969–979.

601 8. Li J, Kreicbergs A, Bergstrom J, Stark A, Ahmed M (2007) Site-specific CGRP innervation
602 coincides with bone formation during fracture healing and modeling: A study in rat
603 angulated tibia. *J Orthop Res* **25**: 1204–1212.

604 9. Gomez C, Burt-Pichat B, Mallein-Gerin F, Merle B, Delmas PD, Skerry TM, Vico L, Malaval
605 L, Chenu C (2005) Expression of Semaphorin-3A and its receptors in endochondral
606 ossification: potential role in skeletal development and innervation. *Dev Dyn* **234**: 393–
607 403.

608 10. Tomlinson RE, Li Z, Zhang Q, Goh BC, Li Z, Thorek DLJ, Rajbhandari L, Brushart TM,
609 Minichiello L, Zhou F, et al. (2016) NGF-TrkA Signaling by Sensory Nerves Coordinates the
610 Vascularization and Ossification of Developing Endochondral Bone. *Cell Rep* 1–13.

611 11. Chartier SR, Thompson ML, Longo G, Fealk MN, Majuta LA, Mantyh PW (2014) Exuberant
612 sprouting of sensory and sympathetic nerve fibers in nonhealed bone fractures and the
613 generation and maintenance of chronic skeletal pain. *Pain* **155**: 2323–2336.

614 12. Bloom AP, Jimenez-Andrade JM, Taylor RN, Castañeda-Corral G, Kaczmarska MJ, Freeman
615 KT, Coughlin KA, Ghilardi JR, Kuskowski MA, Mantyh PW (2011) Breast cancer-induced
616 bone remodeling, skeletal pain, and sprouting of sensory nerve fibers. *J Pain* **12**: 698–711.

617 13. Mach DB, Rogers SD, Sabino MC, Luger NM, Schwei MJ, Pomonis JD, Keyser CP, Clohisy
618 DR, Adams DJ, O'Leary P, et al. (2002) Origins of skeletal pain: sensory and sympathetic
619 innervation of the mouse femur. *Neuroscience* **113**: 155–166.

620 14. Jimenez-Andrade JM, Bloom AP, Stake JI, Mantyh WG, Taylor RN, Freeman KT, Ghilardi JR,
621 Kuskowski MA, Mantyh PW (2010) Pathological Sprouting of Adult Nociceptors in Chronic
622 Prostate Cancer-Induced Bone Pain. *J Neurosci* **30**: 14649–14656.

623 15. Jimenez-Andrade JM, Mantyh PW (2012) Sensory and sympathetic nerve fibers undergo
624 sprouting and neuroma formation in the painful arthritic joint of geriatric mice. *Arthritis*
625 *Res Ther* **14**: R101.

626 16. Madsen JE, Hukkanen M, Aune AK, Basran I, Moller JF, Polak JM, Nordsletten L (1998)
627 Fracture healing and callus innervation after peripheral nerve resection in rats. *Clin Orthop*
628 *Relat Res* 230–240.

629 17. Nordsletten L, Madsen JE, Almaas R, Rootwelt T, Halse J, Konttinen YT, Hukkanen M,
630 Santavirta S (1994) The neuronal regulation of fracture healing. Effects of sciatic nerve
631 resection in rat tibia. *Acta Orthop Scand* **65**: 299–304.

632 18. Li J, Ahmad T, Spetea M, Ahmed M, Kreicbergs A (2001) Bone reinnervation after fracture:
633 a study in the rat. *J Bone Min Res* **16**: 1505–1510.

634 19. Song D, Jiang X, Zhu S, Li W, Khadka A, Hu J (2012) Denervation impairs bone regeneration
635 during distraction osteogenesis in rabbit tibia lengthening. *Acta Orthop* **83**: 406–410.

636 20. Cherruau M, Facchinetti P, Baroukh B, Saffar JL (1999) Chemical sympathectomy impairs
637 bone resorption in rats: a role for the sympathetic system on bone metabolism. *Bone* **25**:
638 545–551.

639 21. Edoff K, Hellman J, Persliden J, Hildebrand C (1997) The developmental skeletal growth in
640 the rat foot is reduced after denervation. *Anat Embryol (Berl)* **195**: 531–538.

641 22. Hill EL, Elde R (1991) Distribution of CGRP-, VIP-, D beta H-, SP-, and NPY-immunoreactive
642 nerves in the periosteum of the rat. *Cell Tissue Res* **264**: 469–480.

643 23. Bove SE, Flatters SJL, Inglis JJ, Mantyh PW (2009) New advances in musculoskeletal pain.
644 *Brain Res Rev* **60**: 187–201.

645 24. Fukuda T, Takeda S, Xu R, Ochi H, Sunamura S, Sato T, Shibata S, Yoshida Y, Gu Z, Kimura
646 A, et al. (2013) Sema3A regulates bone-mass accrual through sensory innervations. *Nature*
647 **497**: 490–493.

648 25. Hayashi M, Nakashima T, Taniguchi M, Kodama T, Kumanogoh A, Takayanagi H (2012)
649 Osteoprotection by semaphorin 3A. *Nature* **485**: 69–74.

650 26. Jones KB, Mollano A V, Morcuende J a, Cooper RR, Saltzman CL (2004) Bone and brain: a
651 review of neural, hormonal, and musculoskeletal connections. *Iowa Orthop J* **24**: 123–132.

652 27. Lee Y, Kim HJ, Park CK, Kim W-S, Lee ZH, Kim H-H (2012) Novel extraneural role of neurite
653 outgrowth inhibitor A: Modulation of osteoclastogenesis via positive feedback regulation
654 of nuclear factor of activated T cell cytoplasmic 1. *J Bone Miner Res* **27**: 1043–1054.

655 28. Neuhuber B, Timothy Himes B, Shumsky JS, Gallo G, Fischer I (2005) Axon growth and
656 recovery of function supported by human bone marrow stromal cells in the injured spinal
657 cord exhibit donor variations. *Brain Res* **1035**: 73–85.

658 29. Lu P, Jones LL, Tuszynski MH (2005) BDNF-expressing marrow stromal cells support
659 extensive axonal growth at sites of spinal cord injury. *Exp Neurol* **191**: 344–360.

660 30. Brohlin M, Kingham PJ, Novikova LN, Novikov LN, Wiberg M (2012) Aging Effect on
661 Neurotrophic Activity of Human Mesenchymal Stem Cells. *PLoS One* **7**: 67–75.

662 31. Novikova LN, Brohlin M, Kingham PJ, Novikov LN, Wiberg M (2011) Neuroprotective and
663 growth-promoting effects of bone marrow stromal cells after cervical spinal cord injury in
664 adult rats. *Cytotherapy* **13**: 873–887.

665 32. Chen X, Katakowski M, Li Y, Lu D, Wang L, Zhang L, Chen J, Xu Y, Gautam S, Mahmood A,
666 et al. (2002) Human bone marrow stromal cell cultures conditioned by traumatic brain
667 tissue extracts: Growth factor production. *J Neurosci Res* **69**: 687–691.

668 33. Gu Y, Wang J, Ding F, Hu N, Wang Y, Gu X (2010) Neurotrophic actions of bone marrow
669 stromal cells on primary culture of dorsal root ganglion tissues and neurons. *J Mol*
670 *Neurosci* **40**: 332–341.

671 34. Han S, Wang B, Li X, Xiao Z, Han J, Zhao Y, Fang Y, Yin Y, Chen B, Dai J (2016) Bone marrow-
672 derived mesenchymal stem cells in three-dimensional culture promote neuronal
673 regeneration by neurotrophic protection and immunomodulation. *J Biomed Mater Res -*
674 *Part A* 1759–1769.

675 35. Wilkins A, Kemp K, Ginty M, Hares K, Mallam E, Scolding N (2009) Human bone marrow-
676 derived mesenchymal stem cells secrete brain-derived neurotrophic factor which
677 promotes neuronal survival in vitro. *Stem Cell Res* **3**: 63–70.

678 36. Ghilardi JR, Freeman KT, Jimenez-Andrade JM, Mantyh WG, Bloom AP, Kuskowski M a,
679 Mantyh PW (2010) Administration of a tropomyosin receptor kinase inhibitor attenuates
680 sarcoma-induced nerve sprouting, neuroma formation and bone cancer pain. *Mol Pain* **6**:

681 87.

682 37. Middlemiss T, Laird BJA, Fallon MT (2011) Mechanisms of Cancer-induced Bone Pain. *Clin*
683 *Oncol* **23**: 387–392.

684 38. Mantyh PW (2014) The neurobiology of skeletal pain. *Eur J Neurosci* **39**: 508–519.

685 39. Yoneda T, Hata K, Nakanishi M, Nagae M, Nagayama T, Wakabayashi H, Nishisho T, Sakurai
686 T, Hiraga T (2011) Involvement of acidic microenvironment in the pathophysiology of
687 cancer-associated bone pain. *Bone* **48**: 100–105.

688 40. Kohno N, Aogi K, Minami H, Nakamura S, Asaga T, Iino Y, Watanabe T, Goessl C, Ohashi Y,
689 Takashima S (2005) Zoledronic Acid Significantly Reduces Skeletal Complications
690 Compared With Placebo in Japanese Women With Bone Metastases From Breast Cancer:
691 A Randomized, Placebo-Controlled Trial. *J Clin Oncol* **23**: 3314–3321.

692 41. Cleeland CS, Body J-J, Stopeck A, von Moos R, Fallowfield L, Mathias SD, Patrick DL,
693 Clemons M, Tonkin K, Masuda N, et al. (2013) Pain outcomes in patients with advanced
694 breast cancer and bone metastases. *Cancer* **119**: 832–838.

695 42. Yoneda T, Hiasa M, Nagata Y, Okui T, White FA (2015) Acidic microenvironment and bone
696 pain in cancer-colonized bone. *Bonekey Rep* **4**: 690.

697 43. Bessa S, Quelhas P, Amaral IF (2013) Automatic Quantification of Cell Outgrowth from
698 Neurospheres. In Sanches JM, Micó L, Cardoso JS (eds.), *Pattern Recognition and Image*
699 *Analysis: 6th Iberian Conference, IbPRIA 2013, Funchal, Madeira, Portugal, June 5-7, 2013.*
700 *Proceedings* pp 141–148. Springer Berlin Heidelberg, Berlin, Heidelberg.

701 44. Gu W, Zhang F, Xue Q, Ma Z, Lu P, Yu B (2012) Bone mesenchymal stromal cells stimulate
702 neurite outgrowth of spinal neurons by secreting neurotrophic factors. *Neurol Res* **34**:
703 172–180.

704 45. Gutierrez H, Kisiswa L, O'Keeffe GW, Smithen MJ, Wyatt S, Davies AM (2013) Regulation
705 of neurite growth by tumour necrosis superfamily member RANKL. *Open Biol* **3**: 120150.

706 46. Imai Y, Kohsaka S (2002) Intracellular signaling in M-CSF-induced microglia activation: Role
707 of Iba1. *Glia* **40**: 164–174.

708 47. Neto E, Alves CJ, Sousa DM, Alencastre IS, Lourenço AH, Leitão L, Ryu HR, Jeon NL,
709 Fernandes R, Aguiar P, et al. (2014) Sensory neurons and osteoblasts: close partners in a
710 microfluidic platform. *Integr Biol* **6**: 586.

711 48. Chao M V (2003) Neurotrophins and their receptors: A convergence point for many
712 signalling pathways. *Nat Rev Neurosci* **4**: 299–309.

713 49. Togari A, Mogi M, Arai M, Yamamoto S, Koshihara Y (2000) Expression of mRNA for axon
714 guidance molecules, such as semaphorin-III, netrins and neurotrophins, in human
715 osteoblasts and osteoclasts. *Brain Res* **878**: 204–209.

716 50. Vigneswara V, Kundi S, Ahmed Z (2012) Receptor tyrosine kinases: molecular switches
717 regulating CNS axon regeneration. *J Signal Transduct* **2012**: 361721.

718 51. Olayioye MA (2000) The ErbB signaling network: receptor heterodimerization in
719 development and cancer. *EMBO J* **19**: 3159–3167.

720 52. Macdonald-Obermann JL, Adak S, Landgraf R, Piwnica-Worms D, Pike LJ (2013) Dynamic
721 analysis of the epidermal growth factor (EGF) receptor-ErbB2-ErbB3 protein network by
722 luciferase fragment complementation imaging. *J Biol Chem* **288**: 30773–30784.

723 53. Mizobuchi S, Kanzaki H (2013) Spinal nerve injury causes upregulation of ErbB2 and ErbB3
724 receptors in rat dorsal root ganglia. *J Pain Res* **6**: 87–94.

725 54. Berry M, Ahmed Z, Douglas MR, Logan A (2011) Epidermal growth factor receptor
726 antagonists and CNS axon regeneration: Mechanisms and controversies. *Brain Res Bull* **84**:
727 289–299.

728 55. Koprivica V, Cho K-S, Park JB, Yiu G, Atwal J, Gore B, Kim J a, Lin E, Tessier-Lavigne M, Chen
729 DF, et al. (2005) EGFR Activation Mediates Inhibition of Axon Regeneration by Myelin and
730 Chondroitin Sulfate Proteoglycans. *Science (80-)* **310**: 106–110.

731 56. Leinster VHL, Joy MT, Vuononvirta RE, Bolsover SR, Anderson PN (2013) ErbB1 epidermal
732 growth factor receptor is a valid target for reducing the effects of multiple inhibitors of
733 axonal regeneration. *Exp Neurol* **239**: 82–90.

734 57. Liu B, Chen H, Johns TG, Neufeld AH (2006) Epidermal Growth Factor Receptor Activation:
735 An Upstream Signal for Transition of Quiescent Astrocytes into Reactive Astrocytes after
736 Neural Injury. *J Neurosci* **26**: 7532–7540.

737 58. Hendry JM, Alvarez-Veronesi MC, Placheta E, Zhang JJ, Gordon T, Borschel GH (2016)
738 ErbB2 blockade with Herceptin (trastuzumab) enhances peripheral nerve regeneration
739 after repair of acute or chronic peripheral nerve injury. *Ann Neurol* **80**: 112–126.

740 59. Tsai N-P, Tsui Y-C, Pintar JE, Loh HH, Wei L-N (2010) Kappa opioid receptor contributes to

741 EGF-stimulated neurite extension in development. *Proc Natl Acad Sci U S A* **107**: 3216–
742 3221.

743 60. Nilsson A, Kanje M (2005) Amphiregulin acts as an autocrine survival factor for adult
744 sensory neurons. *Neuroreport* **16**: 213–218.

745 61. Hynes NE, Lane H a (2005) ERBB receptors and cancer: the complexity of targeted
746 inhibitors. *Nat Rev Cancer* **5**: 341–354.

747 62. Nielsen DL, Kümler I, Palshof JAE, Andersson M (2013) Efficacy of HER2-targeted therapy
748 in metastatic breast cancer. Monoclonal antibodies and tyrosine kinase inhibitors. *The*
749 *Breast* **22**: 1–12.

750 63. Goldshmit Y, Greenhalgh CJ, Turnley AM (2004) Suppressor of cytokine signalling-2 and
751 epidermal growth factor regulate neurite outgrowth of cortical neurons. *Eur J Neurosci*
752 **20**: 2260–2266.

753 64. Wildering WC, Hermann PM, Bulloch AGM (2001) Lymnaea Epidermal Growth Factor
754 Promotes Axonal Regeneration in CNS Organ Culture. *J Neurosci* **21**: 9345–9354.

755 65. Tonge DA, de Burgh HT, Docherty R, Humphries MJ, Craig SE, Pizzey J (2012) Fibronectin
756 supports neurite outgrowth and axonal regeneration of adult brain neurons in vitro. *Brain*
757 *Res* **1453**: 8–16.

758 66. Yoon C, Van Niekerk E a, Henry K, Ishikawa T, Orita S, Tuszynski MH, Campana WM (2013)
759 Low-density lipoprotein receptor-related protein 1 (LRP1)-dependent cell signaling
760 promotes axonal regeneration. *J Biol Chem* **288**: 26557–26568.

761 67. Matsunaga E, Nambu S, Oka M, Tanaka M, Taoka M, Iriki A (2015) Periostin, a neurite
762 outgrowth-promoting factor, is expressed at high levels in the primate cerebral cortex.
763 *Dev Growth Differ* **57**: 200–208.

764 68. Shih C-H, Lacagnina M, Leuer-Bisciotti K, Proschel C (2014) Astroglial-Derived Periostin
765 Promotes Axonal Regeneration after Spinal Cord Injury. *J Neurosci* **34**: 2438–2443.

766 69. Balanis N, Yoshigi M, Wendt MK, Schiemann WP, Carlin CR (2011) β3 integrin-EGF receptor
767 cross-talk activates p190RhoGAP in mouse mammary gland epithelial cells. *Mol Biol Cell*
768 **22**: 4288–4301.

769 70. Morra L, Moch H (2011) Periostin expression and epithelial-mesenchymal transition in
770 cancer: A review and an update. *Virchows Arch* **459**: 465–475.

771 71. Cabodi S, Moro L, Bergatto E, Boeri Erba E, Di Stefano P, Turco E, Tarone G, Defilippi P
772 (2004) Integrin regulation of epidermal growth factor (EGF) receptor and of EGF-
773 dependent responses. *Biochem Soc Trans* **32**: 438–442.

774 72. Clarke B (2008) Normal Bone Anatomy and Physiology. *Clin J Am Soc Nephrol* **3**: S131–
775 S139.

776 73. Sisask G, Bjurholm A, Ahmed M, Kreicbergs A (1996) The development of autonomic
777 innervation in bone and joints of the rat. *J Aut Nerv Syst* **59**: 27–33.

778 74. Gajda M, Litwin J a., Cichocki T, Timmermans JP, Adriaensen D, Timmermanns JP,
779 Adriaensen D (2005) Development of sensory innervation in rat tibia: co-localization of
780 CGRP and substance P with growth-associated protein 43 (GAP-43). *J Anat* **207**: 135–144.

781 75. Reddy S V, Menaa C, Singer FR, Demulder A, Roodman GD (1999) Cell biology of Paget's
782 disease. *J Bone Miner Res* **14 Suppl 2**: 3–8.

783 76. Riminucci M, Kuznetsov SA, Cherman N, Corsi A, Bianco P, Gehron Robey P (2003)
784 Osteoclastogenesis in fibrous dysplasia of bone: In situ and in vitro analysis of IL-6
785 expression. *Bone* **33**: 434–442.

786 77. Cheung MS, Glorieux FH, Rauch F (2009) Large osteoclasts in pediatric osteogenesis
787 imperfecta patients receiving intravenous pamidronate. *J Bone Miner Res* **24**: 669–674.

788 78. Mediati RD, Vellucci R, Dodaro L (2014) Pathogenesis and clinical aspects of pain in
789 patients with osteoporosis. *Clin Cases Miner Bone Metab* **11**: 169–172.

790 79. Nagae M, Hiraga T, Wakabayashi H, Wang L, Iwata K, Yoneda T, Clerck LS De (2006)
791 Osteoclasts play a part in pain due to the inflammation adjacent to bone. *Bone* **39**: 1107–
792 1115.

793 80. Kumar KR, Liang C, Needham M, Burke D, Sue CM, Ng K (2011) Axonal hyperpolarization
794 in inclusion-body myopathy, paget disease of the bone, and frontotemporal dementia
795 (IBMPFD). *Muscle Nerve* **44**: 191–196.

796 81. Julius D, Basbaum AI (2001) Molecular mechanisms of nociception. *Nature* **413**: 203–210.

797 82. Hara-Irie F, Amizuka N, Ozawa H (1996) Immunohistochemical and ultrastructural
798 localization of CGRP-positive nerve fibers at the epiphyseal trabecules facing the growth
799 plate of rat femurs. *Bone* **18**: 29–39.

800 83. Chenu C, Serre CM, Raynal C, Burt-Pichat B, Delmas PD (1998) Glutamate receptors are

801 expressed by bone cells and are involved in bone resorption. *Bone* 22: 295–299.

802 84. Basbaum AI, Bautista DM, Scherrer G, Julius D (2010) Cellular and Molecular Mechanisms
803 of Pain. *NIH Public Access* 139: 267–284.

804 85. Lykissas MG, Batistatou AK, Charalabopoulos K a, Beris AE (2007) The role of
805 neurotrophins in axonal growth, guidance, and regeneration. *Curr Neurovasc Res* 4: 143–
806 151.

807 86. Nakano N, Nakai Y, Seo T-BB, Yamada Y, Ohno T, Yamanaka A, Nagai Y, Fukushima M,
808 Suzuki Y, Nakatani T, et al. (2010) Characterization of conditioned medium of cultured
809 bone marrow stromal cells. *Neurosci Lett* 483: 57–61.

810 87. Kamishina H, Cheeseman J a., Clemmons RM (2009) The effects of canine bone marrow
811 stromal cells on neuritogenesis from dorsal root ganglion neurons in vitro. *Vet Res*
812 *Commun* 33: 645–657.

813 88. Kamei N, Tanaka N, Oishi Y, Ishikawa M, Hamasaki T, Nishida K, Nakanishi K, Sakai N, Ochi
814 M (2007) Bone marrow stromal cells promoting corticospinal axon growth through the
815 release of humoral factors in organotypic cocultures in neonatal rats. *J Neurosurg Spine* 6:
816 412–419.

817 89. Asaumi K, Nakanishi T, Asahara H, Inoue H, Takigawa M (2000) Expression of
818 neurotrophins and their receptors (TRK) during fracture healing. *Bone* 26: 625–633.

819 90. Obata K, Furuno T, Nakanishi M, Togari A (2007) Direct neurite-osteoblastic cell
820 communication, as demonstrated by use of an in vitro co-culture system. *FEBS Lett* 581:
821 5917–5922.

822 91. Crigler L, Robey RC, Asawachaicharn A, Gaupp D, Phinney DG (2006) Human mesenchymal
823 stem cell subpopulations express a variety of neuro-regulatory molecules and promote
824 neuronal cell survival and neuritogenesis. *Exp Neurol* 198: 54–64.

825 92. Cantinieaux D, Quertainmont R, Blacher S, Rossi L, Wanet T, Noël A, Brook G, Schoenen J,
826 Franzen R (2013) Conditioned Medium from Bone Marrow-Derived Mesenchymal Stem
827 Cells Improves Recovery after Spinal Cord Injury in Rats: An Original Strategy to Avoid Cell
828 Transplantation. *PLoS One* 8:.

829 93. Batchelor PE, Porritt MJ, Martinello P, Parish CL, Liberatore GT, Donnan G a, Howells DW
830 (2002) Macrophages and Microglia Produce Local Trophic Gradients That Stimulate Axonal
831 Sprouting Toward but Not beyond the Wound Edge. *Mol Cell Neurosci* 21: 436–453.

832 94. Vidal PM, Lemmens E, Dooley D, Hendrix S (2013) The role of ' anti-inflammatory'
833 cytokines in axon regeneration. *Cytokine Growth Factor Rev* **24**: 1–12.

834 95. Kigerl KA, Gensel JC, Ankeny DP, Alexander JK, Donnelly DJ, Popovich PG (2009)
835 Identification of Two Distinct Macrophage Subsets with Divergent Effects Causing either
836 Neurotoxicity or Regeneration in the Injured Mouse Spinal Cord. *J Neurosci* **29**: 13435–
837 13444.

838 96. Gensel JC, Nakamura S, Guan Z, van Rooijen N, Ankeny DP, Popovich PG (2009)
839 Macrophages Promote Axon Regeneration with Concurrent Neurotoxicity. *J Neurosci* **29**:
840 3956–3968.

841 97. Su Y, Cui L, Piao C, Li B, Zhao L-R (2013) The Effects of Hematopoietic Growth Factors on
842 Neurite Outgrowth. *PLoS One* **8**: e75562.

843 98. Yin Y, Henzl MT, Lorber B, Nakazawa T, Thomas TT, Jiang F, Langer R, Benowitz LI (2006)
844 Oncomodulin is a macrophage-derived signal for axon regeneration in retinal ganglion
845 cells. *Nat Neurosci* **9**: 843–852.

846 99. Xian CJ, Zhou XF (1999) Neuronal-glial differential expression of TGF-alpha and its receptor
847 in the dorsal root ganglia in response to sciatic nerve lesion. *Exp Neurol* **157**: 317–326.

848 100. Douglas MR, Morrison KC, Jacques SJ, Leadbeater WE, Gonzalez AM, Berry M, Logan A,
849 Ahmed Z (2009) Off-target effects of epidermal growth factor receptor antagonists
850 mediate retinal ganglion cell disinhibited axon growth. *Brain* **132**: 3102–3121.

851 101. Wong RWC, Guillaud L (2004) The role of epidermal growth factor and its receptors in
852 mammalian CNS. *Cytokine Growth Factor Rev* **15**: 147–156.

853 102. Neto E, Alves CJ, Leitão L, Sousa DM, Alencastre IS, Conceição F, Lamghari M (2017) Axonal
854 outgrowth, neuropeptides expression and receptors tyrosine kinase phosphorylation in
855 3D organotypic cultures of adult dorsal root ganglia. *PLoS One* **12**: e0181612.

856 103. Xu M, Zhou H, Hu C, Liang Y, Hu L, Chen D (2014) The mechanisms of EGFR in the regulation
857 of axon regeneration. 101–105.

858 104. Evangelopoulos ME, Weis J, Krüttgen A (2009) Mevastatin-induced neurite outgrowth of
859 neuroblastoma cells via activation of EGFR. *J Neurosci Res* **87**: 2138–2144.

860 105. Goldshmit Y, Walters CE, Scott HJ, Greenhalgh CJ, Turnley AM (2004) SOCS2 induces
861 neurite outgrowth by regulation of epidermal growth factor receptor activation. *J Biol*

862 *Chem* **279**: 16349–16355.

863 106. Ahmed Z, Jacques SJ, Berry M, Logan A (2009) Epidermal growth factor receptor inhibitors
864 promote CNS axon growth through off-target effects on glia. *Neurobiol Dis* **36**: 142–150.

865 107. Bartell SM, Kim H-N, Ambrogini E, Han L, Iyer S, Serra Ucer S, Rabinovitch P, Jilka RL,
866 Weinstein RS, Zhao H, et al. (2014) FoxO proteins restrain osteoclastogenesis and bone
867 resorption by attenuating H2O2 accumulation. *Nat Commun* **5**: 3773.

868 108. Sousa DM, Conceição F, Silva DI, Leitão L, Neto E, Alves CJ, Alencastre IS, Herzog H, Aguiar
869 P, Lamghari M (2016) Ablation of Y1 receptor impairs osteoclast bone-resorbing activity.
870 *Sci Rep* **6**: 33470.

871